Journal of Power Sources 239 (2013) 332–340

Contents lists available at SciVerse ScienceDirect

Journal of Power Sources

journal homepage: www.elsevier.com/locate/jpowsour

Composite cathode based on Fe-loaded LSCM for steam electrolysis in an oxide-ion-conducting solid oxide electrolyser

Shanshan Xu [a], Shigang Chen [a], Meng Li [a], Kui Xie [a,b,*], Yan Wang [a], Yucheng Wu [a,b,*]

[a] Department of Energy Materials, School of Materials Science and Engineering, Hefei University of Technology, No. 193 Tunxi Road, Hefei, Anhui 230009, China
[b] Key Laboratory of Advanced Functional Materials and Devices, School of Materials Science and Engineering, Hefei University of Technology, No. 193 Tunxi Road, Hefei, Anhui 230009, China

HIGHLIGHTS

- LSCM fuel electrode shows the feasibility of direct steam electrolysis.
- Electrical properties of LSCM are studied and correlated to cell performances.
- The loading of Fe to LSCM significantly improves fuel electrode and cell performances.
- The synergetic effect of Fe and LSCM leads to direct and efficient steam electrolysis.

ARTICLE INFO

Article history:
Received 29 December 2012
Received in revised form
21 March 2013
Accepted 28 March 2013
Available online 8 April 2013

Keywords:
Solid oxide electrolyser
$La_{0.75}Sr_{0.25}Cr_{0.5}Mn_{0.5}O_{3-\delta}$
Steam electrolysis
Fe catalyst

ABSTRACT

Composite cathodes based on $La_{0.75}Sr_{0.25}Cr_{0.5}Mn_{0.5}O_{3-\delta}$ (LSCM) can perform direct steam electrolysis; however, the insufficient electro-catalytic activity still limits the electrode performances and Faradic efficiency. In this work, Fe catalyst is loaded onto an LSCM-based composite fuel electrode and studied for direct steam electrolysis. The dependence of the conductivity of LSCM on temperature and on oxygen partial pressure is investigated and correlated to the cathode performance. The loading of Fe catalysts significantly improved the electrode performance and the Faradic efficiency without the flow of reducing gas over the cathode. The current efficiency is enhanced by 30% and 40% compared to the values with the bare LSCM-based cathode at 800 °C in 3%H_2O/5%H_2/Ar and 3%H_2O/Ar, respectively. The synergetic effect of catalytic-active Fe and redox-stable LSCM leads to excellent stability and better cathode performance for direct steam electrolysis.

1. Introduction

Hydrogen is an environmental-friendly fuel that can be created from renewable energy resources [1–3]. Production of hydrogen has attracted a great deal of interest in recent years, and one of the effective ways to produce clean hydrogen is high-temperature steam electrolysis [4]. A solid oxide electrolyser (SOE), which operates at temperatures ranging from 700 to 1000 °C, is expected to provide the highest efficiency for steam electrolysis [2,5]. A SOE involves the inverse process of a solid oxide fuel cell (SOFC) and is a promising electrochemical device to directly convert electrical energy into chemical energy [3,6–10]. The steam can be electrolysed into hydrogen and oxygen in an oxygen-ion conducting solid oxide electrolyser under external electricity. At the cathode side, H_2O molecules are electrochemically reduced into H_2 under an externally applied potential. The O^{2-} ions are transported through the oxygen-ion conducting electrolyte to the anode compartment, where O_2 gas is formed and released [7,11,12].

Currently, most reports of high-temperature steam electrolysis have been preferentially performed with a Ni/YSZ composite cathode in SOEs [13,14]. However, a significant concentration of H_2 is required to flow over the Ni cermets to avoid the oxidation of Ni to NiO, which would cause a loss of electronic conductivity and electrode failure. In addition, the conventional Ni/YSZ cathode has some disadvantages, such as poor redox cycling [15–18]. The perovskite LSCM was reported to be an active and redox-stable material [19,20] and has attracted a lot of attention in the high-temperature SOFC field. Furthermore, LSCM is a ceramic material that can be used both for the cathodes and the anodes [21] and can work under oxidising and reducing conditions. However, the

* Corresponding authors. Department of Energy Materials, School of Materials Science and Engineering, Hefei University of Technology, No. 193 Tunxi Road, Hefei, Anhui 230009, China.
E-mail addresses: xiekui@hfut.edu.cn (K. Xie), ycwu@hfut.edu.cn (Y. Wu).

0378-7753/$ – see front matter © 2013 Elsevier B.V. All rights reserved.
http://dx.doi.org/10.1016/j.jpowsour.2013.03.182

catalytic activity of the ceramic materials may be a constraint on the improvement of their catalytic performance [22,23]. Irvine et al. recently demonstrated the feasibility of direct steam electrolysis based on an LSCM/SDC cathode, which did not have a flow of reducing gas over the electrode in an oxygen-ion conducting solid oxide electrolyser [2]. Recently, we also demonstrated that the direct electrolysis of CO_2 could produce CO and O_2 in an oxygen-ion conducting solid oxide electrolyser based on LSCM electrode without the flow of reducing gas over it. However, the Faradic current efficiency is restricted by the insufficient electro-catalytic activity of the LSCM ceramic cathode [24]. Therefore, it is necessary to enhance the electro-catalytic activity of the LSCM cathode to improve the performances of the high-temperature steam electrolysis.

In our study, active Fe metal was loaded onto the composite cathode based on LSCM for steam electrolysis in an oxygen-ion conducting solid oxide electrolyser with or without the flow of reducing gas over the cathode. The electrical properties of LSCM were investigated and correlated to the electrode performances. Then, the cathode based on Fe-loaded LSCM was systematically investigated for steam electrolysis at 800 °C while it was supplied with 3%H_2O/5%H_2/Ar and 3%H_2O/Ar.

2. Experimental

$La_{0.75}Sr_{0.25}Cr_{0.5}Mn_{0.5}O_{3-\delta}$ (LSCM) powders were synthesised using a combustion method followed by a heat treatment at 1200 °C for 5 h in air [25–27]. The nitrate solution was prepared by adding La_2O_3, $Sr(NO_3)_2$, $Cr(NO_3)_3\cdot 9H_2O$, $C_4H_6MnO_4\cdot 4H_2O$ and glycine to a nitric acid solution at the correct molar ratios. The LSCM fine powders were obtained by heating the solution on a heating plate until the solution became brown ash. The $Ce_{0.8}Sm_{0.2}O_{2-\delta}$ (SDC) powders were prepared with Sm_2O_3 and $Ce(NO_3)_3\cdot 6H_2O$ using the same method, and the final heat treatment occurred at 800 °C for 2 h in air. The phase formation of the LSCM and SDC powders were confirmed using X-ray diffraction ($Cu_{K\alpha}$, XRD, $2\Theta = 3°$ min^{-1}, D/MAX2500V, Rigaku Corporation, Japan). A proper amount of LSCM powders was pressed into a bar and sintered at 1400 °C for 10 h in air for a conductivity test. The conductivity test of LSCM was performed in air using the DC four-terminal method from 20 to 800 °C, and the conductivity was recorded using an online system with a step size of 0.4 °C. The dependence of the conductivity on the partial oxygen pressure was tested at 800 °C with an oxygen partial pressure that ranged from 0.2 to 10^{-20} atm, which was adjusted by flowing 5%H_2/Ar. The oxygen partial pressure ($\lg P_{O_2}$) and the conductivity were recorded using an online oxygen sensor (1231, ZrO_2-based oxygen sensor, Noveltech, Australia) and an online multi-meter (Keithley 2000, Digital Multimeter, Keithley Instruments. Inc., USA). The LSCM conductivity test was also performed in 5%H_2/Ar with the temperature ranging from 200 to 800 °C.

A group of 2-mm-thick 8YSZ disks were prepared by dry-pressing 8YSZ powders into green disks with a diameter of ~20 mm. Then, the disks were sintered in air at 1450 °C for 10 h. The two surfaces of the obtained YSZ electrolyte were mechanically polished and ultrasonically cleaned in ethanol and distilled water. The composite electrode LSCM/SDC slurry was prepared by milling the SDC powders with the LSCM powder at a 35:65 weight ratio in alpha-terpineol with a cellulose additive. The electrolysers were prepared by printing the LSCM/SDC electrode slurry onto the YSZ electrolyte in symmetric positions with an area of 1 cm^2, and the process was followed by a heat treatment at 1100 °C for 3 h in air. The cathode with 10 mol% Fe was prepared using an impregnation method with added $Fe(NO_3)_3$ solution. The existence of the Fe element in the LSCM/SDC electrode material was proven by XRD, SEM and EDX. The current collection layer was constructed using silver paste (SS-8060, Xinluyi, Shanghai, China), which was painted onto both electrode surfaces. The external circuit was produced with a silver electrical wire (0.1 mm in diameter), which was connected to the current collectors using silver paste (DAD87, Shanghai Research Institute for Synthetic Resins) and heating at 550 °C for 30 min in air. Scanning electron microscopy (SEM, JEOL Ltd, Japan) was performed to characterise the microstructure of the electrolysers.

The symmetric cells based on the LSCM/Fe/SDC fuel electrode and the LSCM/SDC electrodes were prepared as described in [24]. The AC impedance of the two kinds of symmetric cells was tested with a series of passing current densities in 5%H_2/Ar at 800 °C using an electrochemical station (IM6, Zahner, Germany). All flow rates of the gases were controlled at the rate of 40 ml min^{-1} using a mass flow meter (D08-3F, Sevenstar, Beijing, China). For the steam electrolysis, the single solid oxide electrolyser was sealed to a homemade testing jig using ceramic paste (JD-767, Jiudian, Dongguan, China) for electrochemical measurements. The steam electrolysis in the solid oxide electrolyser based on the LSCM/Fe/SDC and LSCM/SDC composite cathodes was tested under different external potential loads at 800 °C in 3%H_2O/5%H_2/Ar and 3%H_2O/Ar, respectively. The AC impedance spectroscopy and the current-versus-voltage curve (I–V curve) of the SOEs were recorded when the cathodes were exposed to the flowing stream and the anodes were exposed to static air at 800 °C. The steam electrolysis was performed at 1.0, 1.3, 1.5, 1.8 and 2.0 V with the prepared SOEs at 800 °C. The hydrogen concentration of the output gas from the cathode was analysed using an online gas chromatograph (GC9790II, Fuli, Zhejiang, China).

3. Results and discussion

The $La_{0.75}Sr_{0.25}Cr_{0.5}Mn_{0.5}O_{3-\delta}$ (LSCM) and $Ce_{0.8}Sm_{0.2}O_{2-\delta}$ (SDC) powders were prepared via a combustion method followed by a heat treatment at 1200 °C and 800 °C in air, respectively. The XRD patterns of the LSCM and SDC powders were obtained, and Rietvield refinements were performed using the GSAS software. Fig. 1(a) shows the XRD Rietveld refinement of the prepared LSCM sample, which has strong peaks that correspond to the space group R-3c (a = 0.549914 nm; b = 0.549914 nm; c = 1.332281 nm; $\alpha = 90°$; $\beta = 90°$; $\gamma = 120°$). The refinement of the LSCM sample provided the χ^2, wR_p and R_p values of 2.686, 0.1857 and 0.0894, respectively, which indicated a good fit to the experimental data. Fig. 1(b) shows the XRD Rietveld refinement of the SDC sample, which indicated a cubic phase with $a = b = c = 0.543159$ nm and $\alpha = \beta = \gamma = 90°$. The refinement of the SDC sample provided χ^2, wR_p and R_p values of 3.060, 0.1485 and 0.0753, respectively. The two Rietvield refinement images show that both the LSCM and SDC powders are in pure phases.

The perovskite LSCM is a p-type electronic conductor, which can be observed from the dependence of the conductivity on temperature and oxygen partial pressure. Fig. 2(a) shows the dependences of the conductivity of LSCM on temperature in air and in 5%H_2/Ar. In air, a positive temperature coefficient with the activation energy (ΔE) of 26 kJ mol^{-1} was observed for the conductivity. The conductivity increased with the temperature and finally reached approximately 9 S cm^{-1} in air at 800 °C. Similarly, in hydrogen, the conductivity reached 2 S cm^{-1} at 800 °C in air, and the activation energy (ΔE) was approximately 40 kJ mol^{-1}. The p-type conducting behaviour was also observed in Fig. 2(b). The conductivity of the LSCM was independent of the oxygen partial pressure at 800 °C when the oxygen partial pressure was above 10^{-14} atm. However, it significantly decreased when the oxygen partial pressure was below 10^{-14} atm. The low oxygen partial pressure decreased the

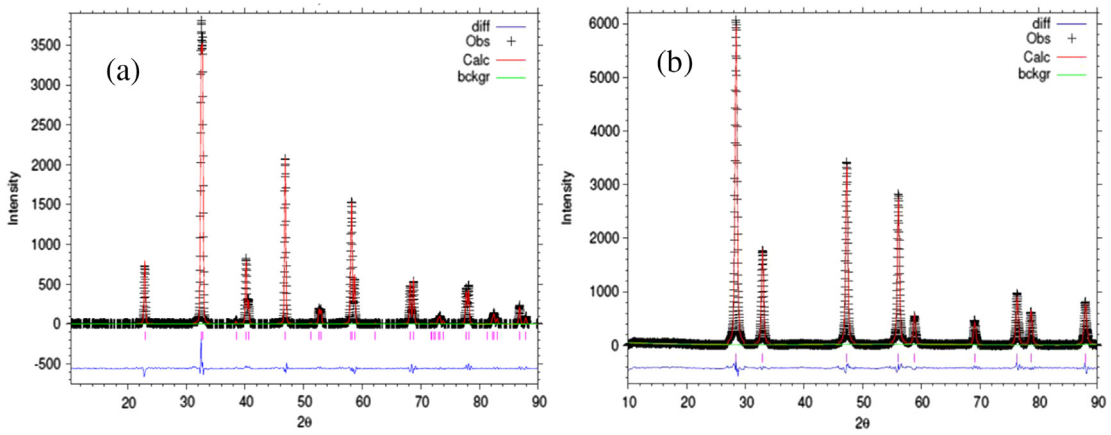

Fig. 1. XRD of the (a) $La_{0.75}Sr_{0.25}Cr_{0.5}Mn_{0.5}O_{3-\delta}$ (LSCM) and (b) $Ce_{0.8}Sm_{0.2}O_{2-\delta}$ (SDC) ceramic powders prepared using the combustion method followed by a heat treatment at 1200 °C for 5 h and 800 °C for 2 h, respectively.

concentration of the charge carrier and the hole in the LSCM ceramic, which is expected to degrade the p-type conductivity. It was observed that the oxygen partial pressure could effectively influence the conductivity of the LSCM ceramic, which might be demonstrated in the form of electrode polarisation during the steam electrolysis in the SOE.

Fig. 3 shows the SEM images of the electrolyte-support SOEs with LSCM/Fe/SDC and LSCM/SDC electrodes. Both LSCM/Fe/SDC and LSCM/SDC composite electrodes appeared to have porous structures and adhered to the dense YSZ electrolyte notably well. The porous silver current collector layer is approximately 2 μm in thickness. The electrochemical performance of the symmetric cells with the configuration of LSCM/Fe/SDC-YSZ-LSCM/Fe/SDC was investigated at 800 °C with two electrodes, which were exposed to the atmosphere of 5%H_2/Ar. The AC impedance data were recorded under a series of applied current densities, as shown in Fig. 4. The intercept of the impedance spectra with the real axis at high frequency corresponds to the Ohmic resistance (R_s) of the cell, which mainly resulted from the ionic resistance of the YSZ electrolyte [28]. Although a slight change was observed at higher current densities, which was probably due to the p-type conduction in the YSZ electrolyte, the Ohmic resistance was reasonable and almost stable (approximately 3.1 Ω cm^2). The electrode polarisation resistance (R_p) was decided using the two intercepts between the imaginary part and the real part at high frequency and low frequency. The values of R_p were obtained by simulating the impedance data using the ZIVEW software. As shown in Figs. 4(a) and (c), there was almost no difference in R_p between the symmetric cells that were based on the LSCM/Fe/SDC composite electrodes and those that were based on the LSCM/SDC composite electrodes, which had current densities below 20 mA cm^{-2} and R_p values above 5 Ω cm^2. However, an obvious change was observed between the two kinds of symmetric cells when the current densities were above 50 mA cm^{-2}. The polarisation resistance R_p of the symmetric cell based on the LSCM/Fe/SDC electrode significantly decreased to approximately 1.9 Ω cm^2 when the current density was under 150 mA cm^{-2}, while the LSCM/SDC electrode achieved only 3 Ω cm^2 under the same conditions, as shown in Figs. 4(b) and (d). This difference indicates that the Fe catalyst effectively enhances the electro-catalytic properties of LSCM and improves the polarisation resistance when the current passes through the electrodes.

The steam electrolysis was investigated in the SOEs, which had the configuration of (cathode) LSCM/Fe/SDC-YSZ-LSCM/SDC (anode) and LSCM/SDC-YSZ-LSCM/SDC at 800 °C with 3%H_2O/5%H_2/Ar and 3%H_2O/Ar supplied to the cathodes, respectively. Fig. 5(a) and (b) shows the typical voltage-versus-current density (I–V curves) of the electrolysers with 3%H_2O/5%H_2/Ar and 3%H_2O/Ar, respectively. The open-circuit voltage (OCV) of the electrolyser was approximately 0.9 V and 0.15 V in 3%H_2O/5%H_2/Ar and 3%H_2O/Ar, respectively, and both values were reasonable according to the

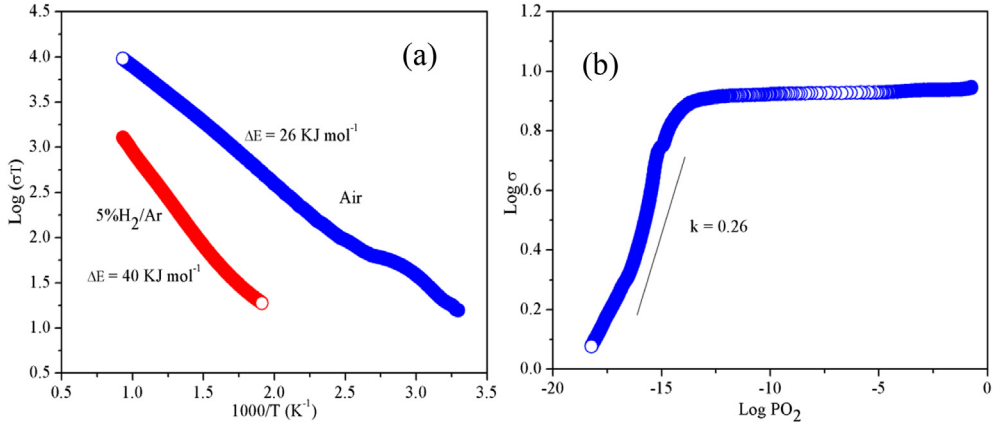

Fig. 2. The dependence of the conductivity of $La_{0.75}Sr_{0.25}Cr_{0.5}Mn_{0.5}O_{3-\delta}$ (LSCM) on (a) the temperature in air from room temperature to 800 °C and in 5%H_2/Ar from 800 to 200 °C and (b) oxygen partial pressure ranging from 0.2 to 10^{-20}atm at 800 °C.

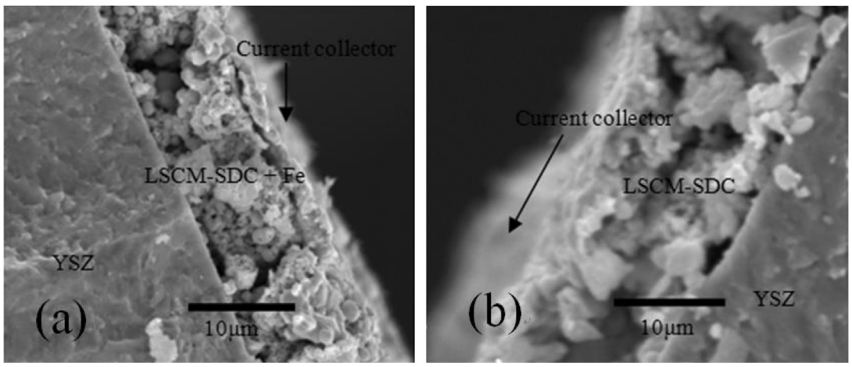

Fig. 3. SEM images of the solid oxide electrolyser with the (a) LSCM/Fe/SDC composite electrode and (b) LSCM/SDC composite electrode.

oxygen concentration cells [2]. The relationship between the current and the voltage is far from linear because the gradient significantly decreased as the current density increased. An obvious change in slope was observed at approximately 1.1 V, which was the anticipated onset potential of H_2 generation from the steam electrolysis. The slope of the *I–V* curves above 1.1 V is lower than that at low voltages, which indicates that there exist two different cell processes in the two voltage regions: (a) steam electrolysis at high voltages and (2) electrochemical reduction of the LSCM cathode and oxidation of the LSCM anode at low voltages. As shown in Fig. 5(a), the current density reached 0.11 A cm^{-2} at 2 V for the LSCM/Fe/SDC cathode in 3%H_2O/5%H_2/Ar, while it only reached 0.09 A cm^{-2} for the LSCM/SDC cathode. This result is consistent with the above discussion about symmetrical cell performance, where the loading of Fe metal significantly improves the electrode performance. Similarly, as shown in Fig. 5(b), the current density reached 0.10 A cm^{-2} at 2 V in 3%H_2O/Ar with the LSCM/Fe/SDC cathode. However, only 0.085 A cm^{-2} was achieved with the LSCM/SDC cathode, which further confirms that the Fe catalyst effectively improves the cathode performance in 3%H_2O/Ar. Nonetheless, it

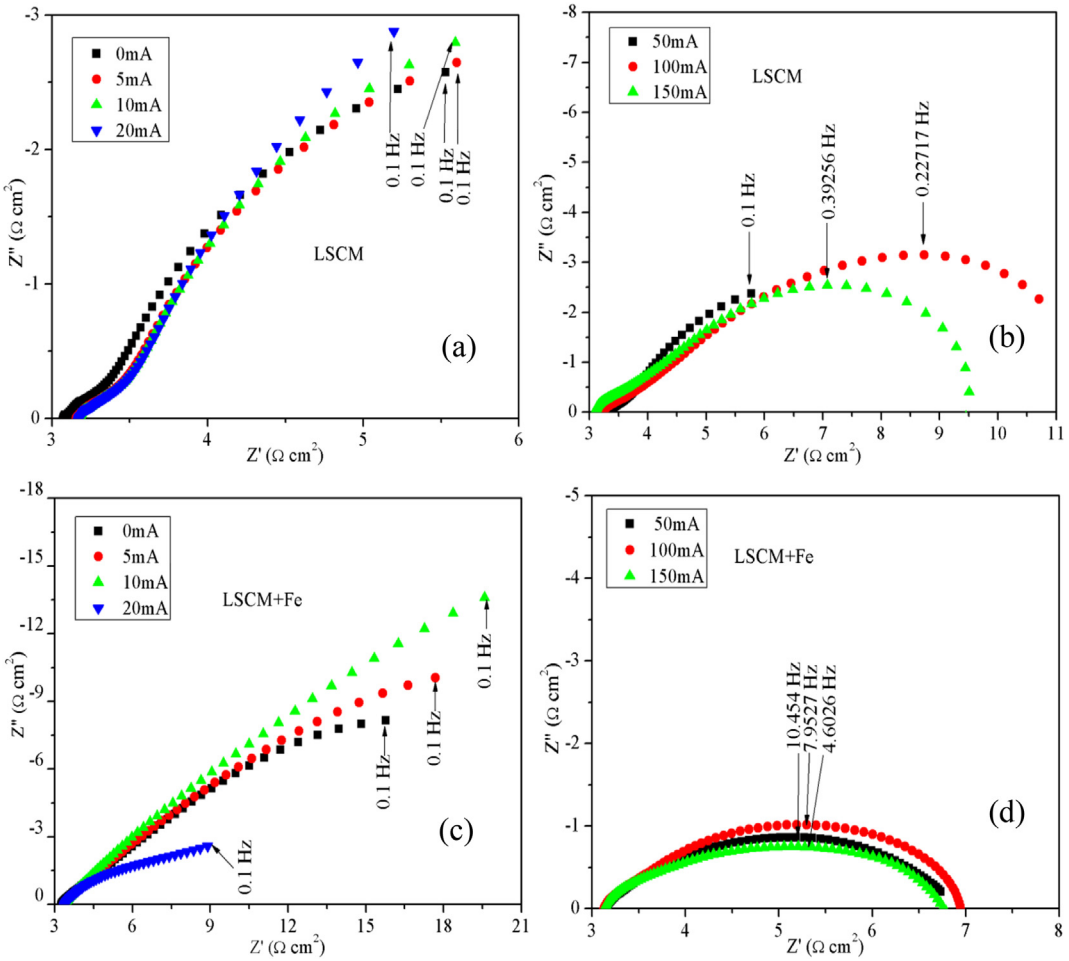

Fig. 4. AC impendence of the symmetric cells LSCM/Fe/SDC-YSZ-LSCM/Fe/SDC and LSCM/SDC-YSZ-LSCM/SDC at 800 °C in 5%H_2/Ar at different current densities.

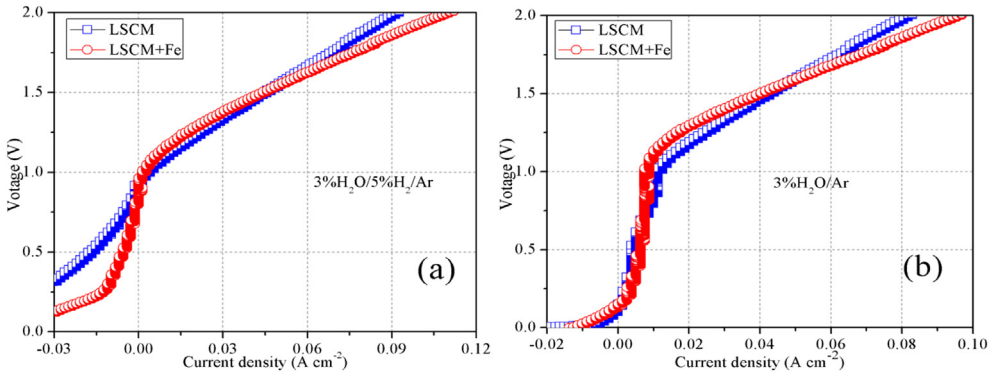

Fig. 5. Current–voltage (I–V) curves of the electrolysers LSCM/Fe/SDC-YSZ-LSCM/SDC and LSCM/SDC-YSZ-LSCM/SDC at 800 °C with 3%H_2O/5%H_2/Ar and 3%H_2O/Ar supplied to the fuel electrode and the oxygen electrode, respectively. The electrodes were exposed to air.

should be noted that the current densities based on LSCM/Fe/SDC in 3%H_2O/5%H_2/Ar were slightly higher than that in 3%H_2O/Ar, which might be related to the better electro-catalytic performance of the cathode in stronger reducing atmospheres.

Figs. 6 and 7 show the *in situ* AC impedance of SOE under a series of external voltages, which ranged from OCV to 2.0 V at 800 °C in 3% H_2O/5%H_2/Ar and 3%H_2O/Ar, respectively. The electrode polarisation resistance, R_p, was considerably large under the low voltages, as shown in Fig. 6(a) and (c). However, the increased voltage significantly activated the electrodes and made the R_p decrease remarkably, which is consistent with the previously discussed result concerning electrode activations in Fig. 5. In Fig. 6(d), the R_p value with Fe-loaded LSCM reached 5 Ω cm^2 at 1.5 V and 4 Ω cm^2 at 1.8 V and further decreased to 3 Ω cm^2 at 2.0 V in 3%H_2O/5%H_2/Ar, while only approximately 5 Ω cm^2 was achieved with the LSCM electrode, as shown in Fig. 6(b) and (d). This result further indicates that the Fe catalyst enhances the catalytic activity of LSCM. Promising electrochemical performance was also observed in the atmosphere of 3%H_2O/Ar, as shown in Fig. 7. The polarisation resistance R_p decreased to 2.5 Ω cm^2 at 2.0 V with the LSCM/Fe/SDC cathode, which was slight smaller than in that in 3%H_2O/5%H_2/Ar. In summary, promising polarisation impedance data were obtained with external voltages for the LSCM/Fe/SDC electrodes in both atmospheres, especially in the gas without the flow of H_2 over the cathode. A possible explanation for this result is that the less reducing atmosphere in 3%H_2O/Ar (compared to 3%H_2O/5%H_2/Ar) led to better mixed p-type conductivity in the LSCM electrodes.

To understand the electrode process, the AC impedance data at 1.5 V in 3%H_2O/Ar with the LSCM/SDC and LSCM/Fe/SDC electrodes were modelled using an equivalent circuit. As shown in Fig. 8(a),

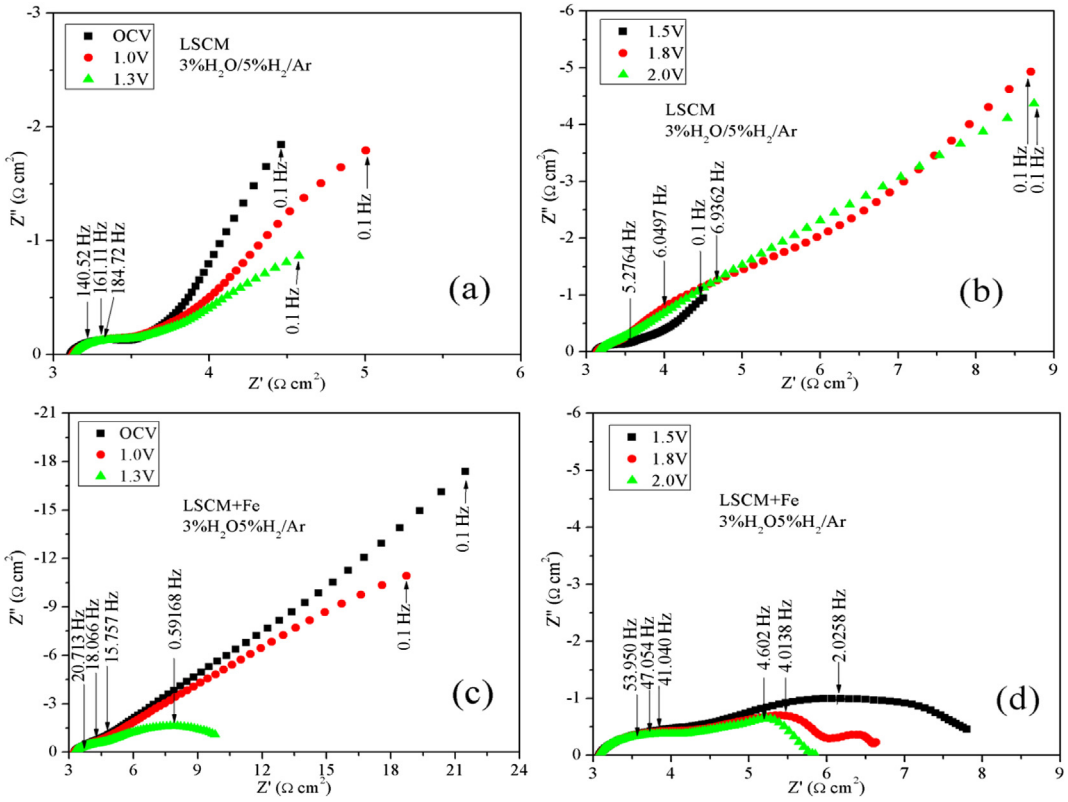

Fig. 6. AC impendence of the electrolyser LSCM/Fe/SDC-YSZ-LSCM/SDC and LSCM/SDC-YSZ-LSCM/SDC at different voltages in 3%H_2O/5%H_2/Ar at 800 °C.

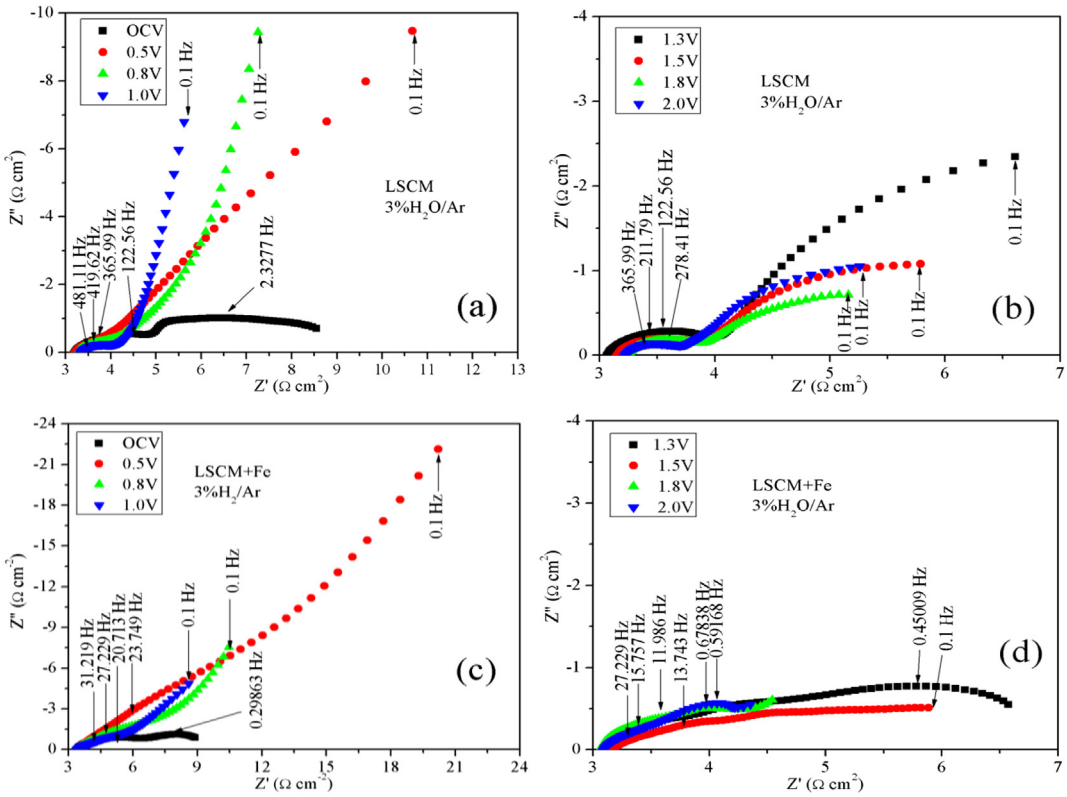

Fig. 7. AC impendence of the electrolyser LSCM/Fe/SDC-YSZ-LSCM/SDC and LSCM/SDC-YSZ-LSCM/SDC at different applied voltages in 3%H_2O/Ar at 800 °C.

the electrode process was assumed to be two arcs, with the equivalent circuits inserted in the figure. The R_1 value was 0.59435 Ω cm^2 for the bare LSCM electrode, which implies a high-frequency process and reflects the charge transfer between LSCM and YSZ. The R_2 value reached 1.664 Ω cm^2, which implies a low-frequency process and reflects the dissociative adsorption, the transfer of species at TPB and the surface diffusion [29,30]. In contrast to the bare LSCM case, for the Fe-loaded LSCM electrode, the R_1 value was 0.43422 Ω cm^2, and the R_2 reaches 1.522 Ω cm^2, as shown in Fig. 8(b), which indicates that the loading of Fe metal improves the mixed conductivity (indicated by the high-frequency process) and the dissociative adsorption, transfer of species at TPB and surface diffusion (indicated by the low-frequency process). Two primary electrochemical processes appeared in the range from OCV to 2 V during the steam electrolysis process: reduction of the LSCM cathode and steam electrolysis. The reduction of the LSCM cathode was the main process below 1.0 V, and the steam electrolysis dominated the electrolysis process at high voltage because the electrochemical potential of $2H_2 + O_2 \rightarrow 2H_2O$ was approximately 1.0 V at 800 °C. At this stage, the R_s value dominated the total cell performance at high voltage, which indicates that the ionic transport in the YSZ electrolyte is the limiting step in the cell process. The electrochemical reduction of the fuel electrode was the main process below an applied electrical voltage of 1.0 V, while the steam electrolysis should be the dominating process above 1.0 V; however, the electrochemical reduction of the LSCM cathode still existed at high voltages.

To further understand the performance of the steam electrolysis process, the current densities were recorded versus time with applied voltages of 1.0 V, 1.3 V, 1.5 V, 1.8 V and 2.0 V. The short-term

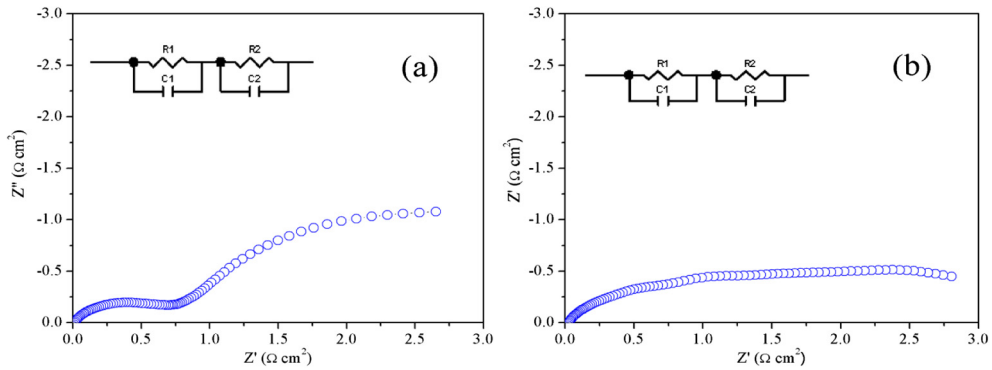

Fig. 8. Models of the in situ AC impedance of the solid oxide electrolyser for steam electrolysis at 1.5 V in 3%H_2O/Ar with (a) LSCM/SDC and (b) LSCM/Fe/SDC fuel electrodes at 800 °C.

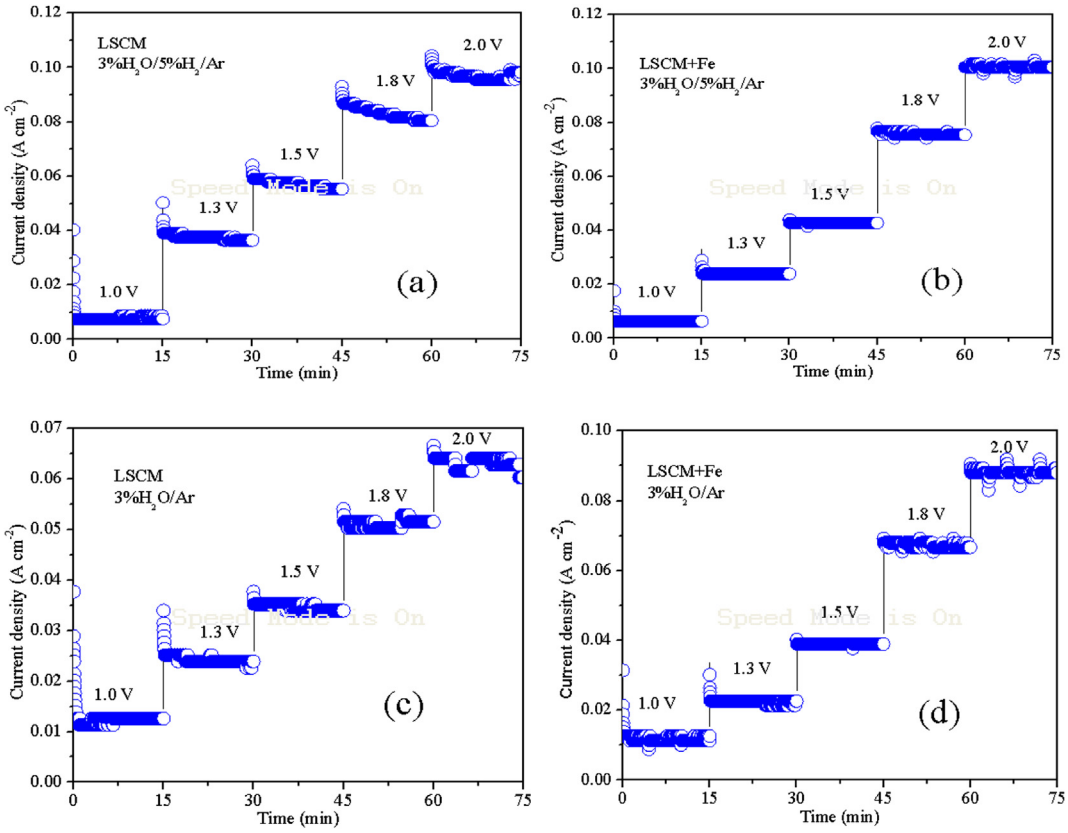

Fig. 9. Performance of the electrolysers LSCM/Fe/SDC-YSZ-LSCM/SDC and LSCM/SDC-YSZ-LSCM/SDC for steam electrolysis under different applied voltages in 3%H_2O/5%H_2/Ar and 3%H_2O/Ar at 800 °C.

performance of both kinds of SOEs for steam electrolysis at 800 °C in atmospheres of 3%H_2O/5%H_2/Ar and 3%H_2O/Ar are shown in Fig. 9(a)–(d), respectively. The current densities were considerably low below 1.0 V, where the electrolysis of H_2O had not started. Fig. 9(a) shows that only 0.04 A cm^{-2} of the current density was obtained at 1.3 V with the LSCM cathode, while the current density was 0.06 A cm^{-2} at 1.5 V and 0.08 A cm^{-2} at 1.8 V. When the applied voltage increased, the current density increased but remained stable under a given potential load. The same results were observed in Fig. 11(b)–(d). The current density reached approximately 0.095 A cm^{-2} at 2.0 V with the bare LSCM fuel electrode, which is lower than 0.10 A cm^{-2} for the Fe-loaded LSCM electrode in 3%H_2O/5%H_2/Ar. On the contrary, the current density with the Fe-loaded LSCM electrode in 3%H_2O/Ar was approximately 0.09 A cm^{-2} at 2.0 V, which is comparable to that in 3%H_2O/5%H_2/Ar but significantly higher than the value 0.06 A cm^{-2} for the bare LSCM electrode under the same condition. The excellent fuel electrode performance in the process of direct steam electrolysis without a flow of reducing gas over the Fe metal was attributed to the synergetic effect of the Fe catalyst and the ceramic LSCM electrode. It can be explained as follows: the hydrogen generated in the fuel electrode protected the catalytic-active Fe metal from oxidation, while the catalyst simultaneously enhanced the electrode performance.

The tested data and the theoretical data of H_2 production from steam electrolysis in the SOE under different applied voltages in 3%H_2O/5%H_2/Ar and 3%H_2O/Ar at 800 °C are shown in Fig. 10(a)–(d), respectively. There was no H_2 production at 1.0 V because the OCV of the H_2-supplied SOFC was above 1.0 V. The hydrogen detection started at 1.3 V. There was an obvious difference between the tested data and the theoretical data for .the LSCM/SDC electrodes in either 3%H_2O/5%H_2/Ar or 3%H_2O/Ar. However, the tested value was close to the theoretical value for the Fe-loaded LSCM electrodes. According to the tested and theoretical data of H_2 production, the current efficiency of the steam electrolysis was obtained as shown in Fig. 11(a) and (b). It is low at low potentials, especially in 3%H_2O/Ar (approximately 20%) for both the bare LSCM and the Fe-loaded LSCM electrodes. However, when the applied voltage increased, the current efficiency also increased. The current efficiency reached 93% and 82% at 2.0 V with the Fe-loaded LSCM fuel electrode, while only 67% and 42% were obtained with the bare LSCM fuel electrodes in 3%H_2O/5%H_2/Ar and 3%H_2O/Ar, respectively. Here, the current efficiency of steam electrolysis was significantly improved when the Fe catalyst was loaded in the fuel electrode. More importantly, according to our short-term test, the synergetic effect of the Fe catalyst and the ceramic LSCM electrode leads to the excellent stability of the fuel electrode in the process of direct steam electrolysis without a flow of reducing gas over the Fe metal.

Fig. 12(a) shows the XRD patterns of Fe-loaded LSCM/SDC before and after the steam electrolysis test at 800 °C. Fe_2O_3 was observed in the cathode before the test. However, Fe_2O_3 was transformed into Fe metal after the test, which confirms the presence of catalytic-active Fe particles in the composite cathode. As shown in Fig. 12(b), SEM and EDX were used together to analyse the cathode surface. It was observed that the Fe element was homogeneously dispersed in the cathode, which was expected to effectively improve the cathode performances. To validate the long-term stability of the composite cathode with Fe-loaded LSCM, direct steam electrolysis was performed at a fixed voltage of 1.5 V for 15 h with Fe-loaded LSCM. As shown in Fig. 13(a), the performance was generally stable in the first hour, which indicates that the short-term performance of the Fe-loaded LSCM is stable. However, a

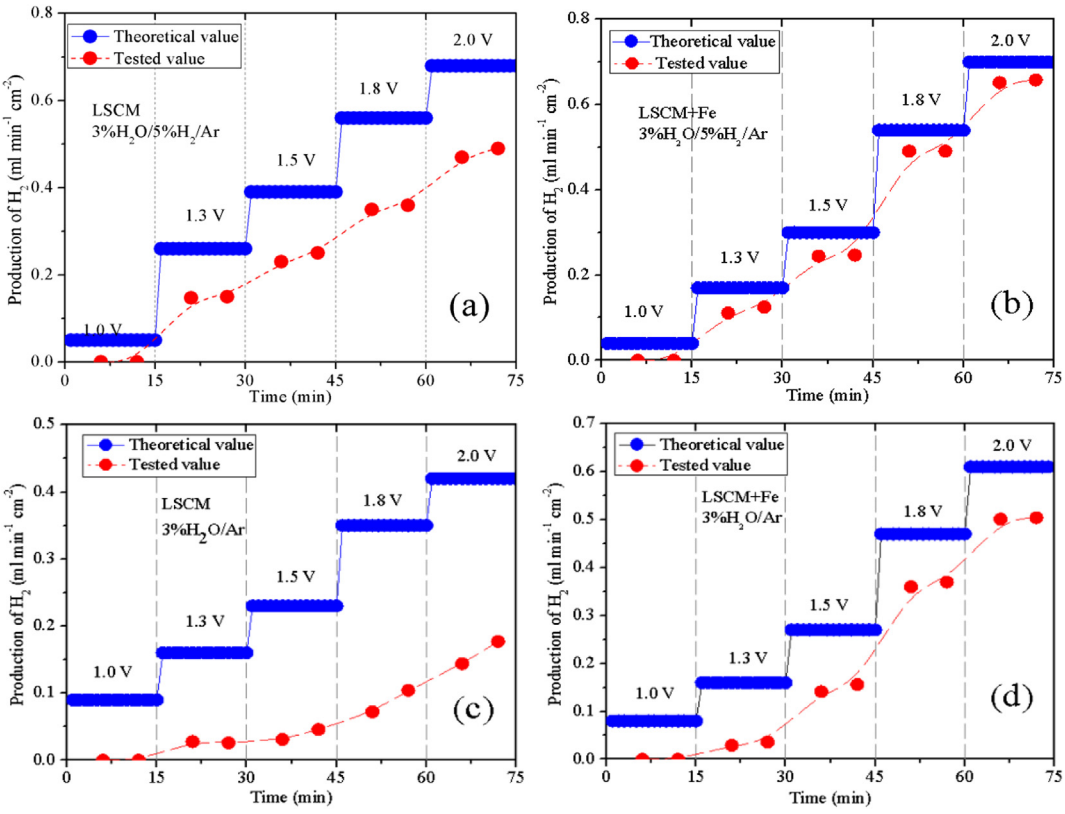

Fig. 10. Production of hydrogen from steam electrolysis in the solid oxide electrolysers LSCM/Fe/SDC-YSZ-LSCM/SDC and LSCM/SDC-YSZ-LSCM/SDC at different applied voltages in 3%H_2O/5%H_2/Ar and 3%H_2O/Ar at 800 °C.

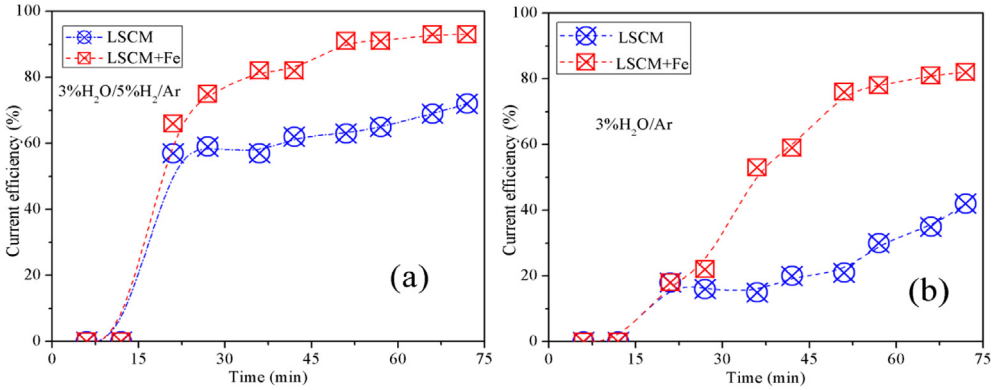

Fig. 11. Faradic current efficiency of steam electrolysis in the solid oxide electrolysers LSCM/Fe/SDC-YSZ-LSCM/SDC and LSCM/SDC-YSZ-LSCM/SDC at different applied voltages in 3% H_2O/5%H_2/Ar and 3%H_2O/Ar at 800 °C.

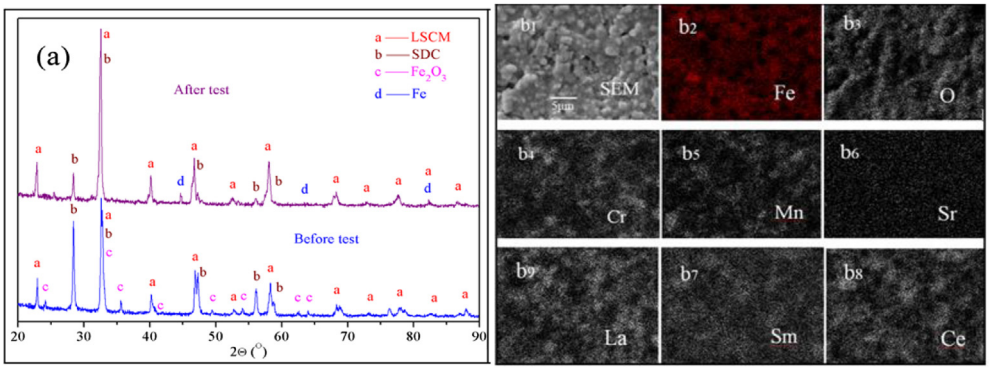

Fig. 12. XRD, SEM and EDX of Fe-loaded $La_{0.75}Sr_{0.25}Cr_{0.5}Mn_{0.5}O_{3-\delta}$/$Ce_{0.8}Sm_{0.2}O_{2-\delta}$ (LSCM/SDC) before and after the test for steam electrolysis at 800 °C.

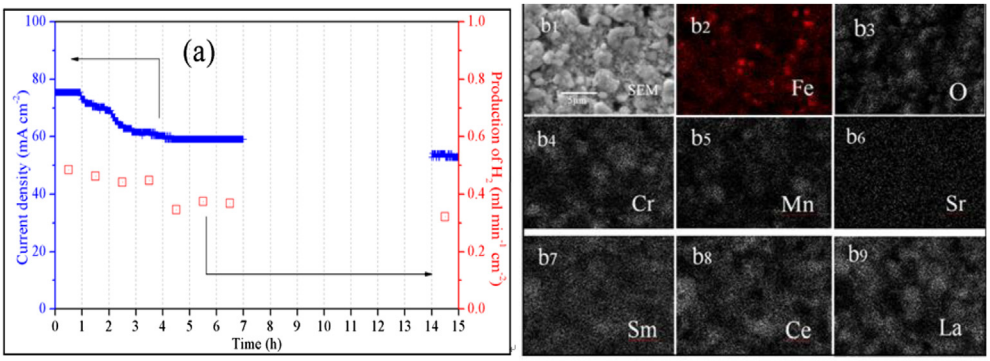

Fig. 13. (a) Long-term performance of the LSCM/Fe/SDC cathode for steam electrolysis at 1.5 V in 3%H_2O/Ar; (b) SEM and EDX of the cathode surface after the long-term test.

decrease of approximately 15–20% was observed after running the direct steam electrolysis for 15 h. To understand the reason, SEM and EDX were used to analyse the cathode surface. Fig. 13(b) shows the agglomeration of Fe particles observed from Fe-element mapping, which could decrease the electro-catalytic activity of the composite cathode, as observed in Fig. 13(a). Therefore, we speculated that it was feasible that preventing the agglomeration of Fe particles at high temperatures would prevent the degradation of the cathode performance.

4. Conclusions

In our work, Fe catalyst was loaded onto a LSCM cathode to improve the catalytic activity for steam electrolysis in an oxygen-ion conducting solid oxide electrolyser. Promising performances were obtained for the solid oxide electrolyser with this cathode when either 3%H_2O/5%H_2/Ar or 3%H_2O/Ar was supplied for the electrolysis at 800 °C. Significant improvements in electrochemical performance and current efficiency were achieved by loading the Fe catalyst onto the LSCM cathode. More importantly, the synergetic effect of the catalytic-active Fe and the redox-stable LSCM made the composite cathode for direct steam electrolysis remarkably stable in the short term. However, the agglomeration of Fe particles degraded the long-term performance of direct steam electrolysis at 800 °C.

References

[1] J.S. Herring, J.E. O'Brien, C.M. Stoots, G.L. Hawkes, J.J. Hartvigsen, M. Shahnam, Int. J. Hydrogen Energy 32 (2007) 440.
[2] X.D. Yang, J.T.S. Irvine, J. Mater. Chem. 18 (2008) 2349.
[3] R.M. Xing, Y.R. Wang, S.H. Liu, C. Jin, J. Power Sources 208 (2012) 276.
[4] M.A. Laguna-Bercero, J.A. Kilner, S.J. Skinner, Solid State Ionics 192 (2011) 501.
[5] A. Hauch, S.D. Ebbesen, S.H. Jensen, M. Mogensen, J. Mater. Chem. 18 (2008) 2333.
[6] T. Ishihara, N. Jirathiwathanakul, H. Zhong, Energy Environ. Sci. 3 (2010) 665.
[7] G. Tsekouras, J.T.S. Irvine, J. Mater. Chem. 21 (2011) 9367.
[8] F. Bidrawn, G. Kim, G. Corre, J.T.S. Irvine, J.M. Vohs, R.J. Gorte, Electrochem. Solid-State Lett. 11 (2008) B167.
[9] B. Yu, W.Q. Zhang, J. Chen, J.M. Xu, S.R. Wang, Sci. China Ser. B-Chem. 51 (2008) 290.
[10] K.F. Chen, N. Ai, S.P. Jiang, Int. J. Hydrogen Energy 37 (2012) 10517.
[11] K. Xie, Y.Q. Zhang, G.Y. Meng, J.T.S. Irvine, Energy Environ. Sci. 4 (2011) 2218.
[12] S.S. Li, Y.X. Li, Y. Gan, K. Xie, G.Y. Meng, J. Power Sources 218 (2012) 244.
[13] S.D. Ebbesen, R. Knibbe, M. Mogensen, J. Electrochem. Soc. 159 (2012) F482.
[14] S.D. Ebbesen, M. Mogensen, J. Power Sources 193 (2009) 349.
[15] S.W. Tao, J.T.S. Irvine, Chem. Mater. 16 (2004) 4116.
[16] J.H. Kim, D. Miller, H. Schlegl, D. McGrouther, J.T.S. Irvine, Chem. Mater. 23 (2011) 3841.
[17] Y. Matsuzaki, I. Yasuda, Solid State Ionics 132 (2000) 261.
[18] D. Sarantaridis, A. Atkinson, Fuel Cells 7 (2007) 246.
[19] S.W. Tao, J.T.S. Irvine, Nat. Mater. 2 (2003) 320.
[20] S.W. Tao, J.T.S. Irvine, S.M. Plint, J. Phys. Chem. 110 (2006) 21771.
[21] S.B. Ha, P.S. Cho, Y.H. Cho, D. Lee, J.H. Lee, J. Power Sources 195 (2010) 124.
[22] G.L. Xiao, C. Jin, Q. Liu, A. Heyden, F.L. Chen, J. Power Sources 201 (2012) 44.
[23] M.D. Gross, K.M. Carver, M.A. Deighan, A. Schenkel, B.M. Smith, A.Z. Yee, J. Electrochem. Soc. 156 (2009) B540.
[24] S.S. Xu, S.S. Li, W.T. Yao, D.H. Dong, K. Xie, J. Power Sources (2012), http://dx.doi.org/10.1016/j.jpowsour.2012.12.068.
[25] H.P. Ding, J.J. Ge, X.J. Xue, B86, Electrochem. Solid-State Lett. 15 (2012).
[26] V.V. Kharton, E.V. Tsipis, I.P. Marozau, A.P. Viskup, J.R. Frade, J.T.S. Irvine, Solid State Ionics 178 (2007) 102.
[27] D.M. Bastidas, S.W. Tao, J.T.S. Irvine, J. Mater. Chem. 16 (2006) 1603.
[28] C. Jin, C.H. Yang, F. Zhao, D. Cui, F.L. Chen, Int. J. Hydrogen Energy 36 (2011) 3340.
[29] M.J. Jorgensen, M. Mogensen, J. Electrochem. Soc. 148 (2001) A433.
[30] Y. Gan, J. Zhang, Y.X. Li, S.S. Li, K. Xie, J.T.S. Irvine, J. Electrochem. Soc. 159 (2012) F763.